Research article

Diphlorethohydroxycarmalol inhibits Müller cell gliosis by disrupting CXCR4/CXCL12 interaction in violet-blue light-induced retinal phototoxicity

Myeongjoo Son [a,b], Dineth Pramuditha Nagahawatta [c], Hang-Chan Jo [d,e], You-Jin Jeon [c,f], Bomi Ryu [g,**], Dae Yu Kim [d,e,h,*]

[a] Department of Anatomy & Cell Biology, School of Medicine, Kangwon National University, Chuncheon, 24341, Republic of Korea
[b] Brain Health Research Laboratory, Institute of Medical Science, Kangwon National University College of Medicine, Chuncheon, 24341, Republic of Korea
[c] Department of Marine Life Sciences, Jeju National University, Jeju, 63243, Republic of Korea
[d] Center for Sensor Systems, Inha University, Incheon, 22212, Republic of Korea
[e] Department of Electrical and Computer Engineering, College of Engineering, Inha University, Incheon, 22212, Republic of Korea
[f] Marine Science Institute, Jeju National University, Jeju, 63333, Republic of Korea
[g] Major of Food Science and Nutrition, Pukyong National University, Busan, 48513, Republic of Korea
[h] Inha Research Institute for Aerospace Medicine, Inha University, Incheon, 22212, Republic of Korea

ARTICLE INFO

ABSTRACT

Müller gliosis is a complex process that impairs the ability of retinal Müller glial cells to respond to various forms of retinal injury or disease, leading to retinal damage. Blue light (BL) exposure is a known cause of retinal damage. In this study, we aimed to investigate the potential of DPHC in inhibiting Müller gliosis in models of BL-exposure.

We conducted in silico binding analysis to evaluate the binding of DPHC to CXCR4. Then, we developed in vitro and in vivo experimental models to assess the effects of DPHC and BL exposure on Müller gliosis using MIO-M1 cells and zebrafish.

Our findings show that DPHC can suppress the Müller gliosis process in BL-exposed MIO-M1 cells in vitro and in BL-exposed zebrafish in vivo. In silico molecular docking, we identified CXCR4 as the target of active site 1 of DPHC. In BL-exposed MIO-M1 cells, DPHC inhibited CXCR4 activity and altered the expression of Müller gliosis markers and NF-κB-related ERK and AKT signaling. In BL-exposed zebrafish, DPHC prevented retinal thickness reduction and inhibited CXCR4 expression and retinal cell apoptosis.

This study suggests that DPHC could be a potential therapeutic agent for retinal diseases involving Müller gliosis. By inhibiting CXCR4 activity, DPHC downregulates the ERK/AKT/NF-κB pathway, reducing retinal cell apoptosis and altered expression of Müller gliosis markers. These findings highlight the potential of natural bioactive compounds for treating various diseases, and further research should investigate the therapeutic potential of DPHC and its derivatives.

* Corresponding author. Center for Sensor Systems, Inha University, Incheon, 22212, Republic of Korea.
** Corresponding author.
E-mail addresses: bmryu@pknu.ac.kr (B. Ryu), dyukim@inha.ac.kr (D.Y. Kim).

1. Introduction

Glial cells play diverse and critical roles in the adult nervous system, including immune defense, maintenance of homeostasis, and support for neurons, which making them central to the pathogenesis of many neurological disorders [1]. In the retina, Müller glial cells (RMGs) are the primary glial cells, extending from the outer to the inner retinal layers, where they provide both structural and metabolic support to photoreceptors and other retinal neurons [2,3]. Although RMGs aid in regulating ion and water balance and contribute neuroprotective functions, these cells can also become reactive in response to various stressors contributing to retinal pathology [4–6]. Among potential stressors, excessive exposure to blue light (BL) is known to damage retinal pigment epithelium (RPE) cells, to induce oxidative stress, and to promote photoreceptor cell death [7–10]. Although BL can regulate circadian rhythms and promote alertness, overexposure particularly at wavelengths between 400 and 440 nm has been linked to pathological changes in the retina, including lipofuscin accumulation and age-related macular degeneration [8,9]. For instance, primary RPE cells produce high levels of hydrogen peroxide and exhibit downregulation of glutathione peroxidase (GPX1) expression specifically at 400 nm, suggesting heightened sensitivity to short-wavelength BL [10].

Excessive BL can also trigger gliosis in Müller cells. Reactive gliosis involves morphological and molecular changes, including increased expression of glial fibrillary acidic protein (GFAP) and glutamine synthetase (GS), as well as cellular hypertrophy [8,11,12]. This heightened gliotic response has been implicated in the progression of various retinal diseases, such as age-related macular degeneration (AMD) and diabetic retinopathy, due in part to elevated inflammation, oxidative stress, and blood vessel growth [13].

C-X-C motif chemokine ligand 12 (CXCL12), also known as stromal cell-derived factor 1 (SDF-1), is a chemokine that acts as a ligand for the G-protein coupled receptor chemokine (C-X-C motif) receptor 4 (CXCR4) [14]. Although initially known for its immune system functions, recent studies have shown that it can also be produced by glial cells and neurons in the brain. Scientific research has highlighted the interconnectedness between the CXCL12/CXCR4-7 system and other neurotransmitter systems within the brain, including GABA, glutamate, opioids, and cannabinoids [15]. CXCL12 and its receptor CXCR4 play critical roles in inflammatory responses and glial activation in the spinal cord, and elevated levels of these molecules have been linked to behaviors [16]. Additionally, the relationship between CXCL12 and gliosis has been investigated. CXCL12 acts as a growth factor for astrocytes, stimulating their proliferation in vitro, which could be linked to pathological conditions like gliosis and malignant transformation. The primary pathway responsible for CXCL12-induced proliferation in astrocytes has been identified as the G-protein– Phosphoinositide 3-kinases (PI3K)– ERK1/2 signaling cascade [17].

Recent research has focused on exploring the potential use of natural products for treating retinal diseases related to Müller cell gliosis. To this end, a study was conducted to investigate the efficacy of diphlorethohydroxycarmalol (DPHC), a natural polyphenolic compound extracted from the brown seaweed *Ishige okamurae*, in preventing BL-induced gliosis. DPHC is a phloroglucinol-based compound including characteristics of phlorotannins. These compounds are composed of repeating units of phloroglucinol (1,3,5-trihydroxybenzene). The specific structure of DPHC includes hydroxyl and ether functional groups, which contribute to its strong anti-inflammatory [18] and anti-oxidant properties [19]. In addition, DPHC has been reported to interact with pro-inflammatory cytokines such as TNF-α [18]. Despite these findings, the therapeutic role of DPHC in retinal diseases remains largely unexplored. Building on this gap, we hypothesized that DPHC could mitigate BL-induced retinal damage by modulating gliotic responses in Müller cells. To test this hypothesis, our study aimed to determine whether DPHC interferes with key inflammatory and stress-related pathways specifically the CXCR4/CXCL12 interaction and its downstream signaling cascades in experimental models of BL-induced retinal phototoxicity. The findings presented here provide novel insights into the potential of DPHC to prevent or alleviate Müller gliosis and, by extension, reduce retinal degeneration.

2. Materials and methods

2.1. In silico binding analysis for DPHC-CXCR4

The receptor preparation and molecular docking were performed using the Discovery Studio software (DS-Client v18.1.100.18065) as described previously [20]. Briefly, the basic structure of CXCR4 was obtained from the protein data bank (PDB ID: 3ODU). Heteroatoms and water molecules were removed and minor adjustments to the protein structure were made using the clean protein tool. The receptor protein was further processed using the prepare protein tool, and the most stable form of the protein was obtained using the minimization tool. The two active sites of CXCR4 were selected based on the ligands available with the crystal structure, the cavities on the receptor, and the PDB site records [21]. The radius of the active site sphere was 15 Å. The 3D structure of DPHC was generated using the ligand preparation tool and hydrogen atoms were also added. Next, the most stable pose was obtained using energy minimization of the ligand. The molecular docking simulation was performed using the automated DS flexible docking program to reveal the most stable pose of DPHC with the selected active sites. Then, the binding affinity of DPHC was calculated using the calculate binding energy tool.

2.2. Experimental models

2.2.1. BL irradiator

The BL irradiator comprised an aluminum housing, diffusing optics, custom light-emitting diode (LED) modules, and a heat sink for temperature management. The arrangement of the components can be adjusted to provide different experimental settings by controlling the distance between the light module and the target. The irradiator was equipped with six lens tubes containing a diffusing

optic lens (DGUV10-220; Thorlabs, NJ, USA), which transforms the overlapped light from the LED array to a gaussian-like spatial beam profile for uniform irradiation at the corresponding scopes of the lens tubes. Each LED module was comprised of three BL LEDs arranged in a triangular configuration, and the diffusers within the lens tubes ensure a diffuse gaussian-like light distribution by bidirectional scattering. The BL LED was mounted on a metal plate printed circuit board (PCB) to promote efficient thermal conduction between the LED and the heat sink for heat dissipation. Although the wavelength range of the LEDs spans from 390 nm to 420 nm, which partially covers the ultraviolet A (UVA) range (315–400 nm), the central and peak wavelengths were located at 405 nm, which is consistent with the characteristics of BL.

2.2.2. BL exposures or CXCL12 induction in cell cultures

Diphlorethohydroxycarmalol (CAS 138529-04-1, purity 98 %) was procured from Aktin Chemical Inc. (Chengdu, China). The immortalized Moorfields/Institute of Ophthalmology-Müller 1 (MIO-M1) cells exhibit characteristics of Müller glial cells [22]. The MIO-M1 cell line was obtained from Dr. G.A. Limb (UCL Institute of Ophthalmology, University of London, UK) through a license agreement with UCLB-XIP, London, UK. The cells were cultured in a CO2 incubator using Dulbecco's Modified Eagle Medium (DMEM; Gibco, Grand Island, NY), supplemented with 10 % fetal bovine serum (FBS; Gibco) and 100 U/ml penicillin/streptomycin (Gibco).

To establish an in vitro model of blue light (BL) exposure, 2×10^6 MIO-M1 cells were seeded in a T-75 culture flask, allowed to reach 90 % confluency, and subsequently washed with phosphate-buffered saline (PBS). The cells were then exposed to BL at an intensity of 10 mW/cm^2 for a duration of 100 min. For the DPHC treatments, MIO-M1 cells were treated with either 5 μM or 10 μM DPHC for 1 d, followed by BL exposure for 100 min. In another in vitro model, CXCL12 induction was achieved by treating MIO-M1 cells with 20 nM recombinant CXCL12 protein (R&D Systems) for 1 d. Prior to the induction of CXCL12 in MIO-M1 cells, DPHC was pre-treated with the cells for 1 d.

2.2.3. BL exposures in zebrafish

Adult zebrafish (*Danio rerio*) were obtained from the Zebrafish Center for Disease Modeling (located in Daejeon, Korea) to establish a BL exposure model. The approximately 3–6-month-old zebrafish were maintained under standard conditions at 28.5 °C under a 14 h light/10 h dark photoperiod. The adult zebrafish were randomly divided into four groups, each consisting of 10 individuals: i) Dark Group: the zebrafish were kept in the dark for 4 h each day for a period of 3 d; ii) BL Group: the zebrafish were exposed to BL for 4 h each day for a period of 3 d; iii) BL + DPHC (5 μM) Group: the zebrafish water was treated with DPHC at a concentration of 5 μM for one day, after which the zebrafish were exposed to BL for 4 h each day for a period of 3 d; iv) BL + DPHC (10 μM) Group: the zebrafish water was treated with DPHC at a concentration of 10 μM for 1 d, after which the zebrafish were exposed to BL for 4 h each day for a period of 3 d. All guidelines for zebrafish husbandry and procedures were approved by the Institutional Animal Care and Use Committee of Inha University (approval no. INHA 221121-844).

2.3. Immunocytochemistry

The MIO-M1 cells (1×10^4) were seeded in an 8-well chamber slide (SPL Life Sciences, Pocheon, Korea). The chamber slides were washed with phosphate-buffered saline (PBS) and fixed with 10 % neutral buffered formalin (NBF) for 20 min. The slides were washed with PBS and incubated with normal animal serum (Vectastain Elite Universal ABC kit; Vector Laboratories, CA, USA) for 1 h at room temperature. Afterward, the slides were incubated with primary antibodies (anti-GFAP, anti-glutamine synthetase, anti-CXCR4, anti-NF-κB, and anti-pNF- κB) and rinsed three times with PBS. The slides were then incubated with the biotinylated antibodies from the ABC kit for 1 h and then incubated with an avidin-biotin complex. Next, the tissue slides were developed with 3, 3′-diaminobenzidine (DAB; Sigma-Aldrich, CA, USA) as a substrate for 1 min, then mounted with 100 % glycerol (Sigma-Aldrich) and visualized via light microscopy (Olympus Optical Co., Tokyo, Japan).

2.4. RNA extraction and cDNA synthesis

RNA extraction and complementary DNA (cDNA) synthesis are crucial steps in gene expression analysis. MIO-M1 cells were combined with 1 mL of TRIzol (Invitrogen, MA, USA). Afterward, the homogenates were mixed with 0.2 mL of chloroform (Invitrogen) and centrifuged at $14,000 \times g$ for 20 min at 4 °C. The aqueous phases were transferred to new tubes, mixed with 0.5 mL of isopropanol (Invitrogen), and centrifuged under the same conditions. The isolated total RNA was purified by washing with 70 % ethanol and dissolved in 10–30 μL of nuclease-free water. The quality and quantity of the RNA samples were assessed using a NanoDrop spectrophotometer (Thermo Scientific, MA, USA) at 260 nm. The RNA samples were treated with RNase-free DNase I (Thermo Scientific) to remove any genomic DNA traces. The purified RNA was then used to synthesize cDNA using a reverse transcription kit (SuperScript III Reverse Transcriptase; Invitrogen) according to the manufacturer's instructions. The generated cDNA was then utilized as a template for quantitative real-time polymerase chain reaction (RT-qPCR) to measure the expression levels of target genes.

2.5. Quantitative real-time polymerase chain reaction

Quantitative real-time polymerase chain reaction (RT-qPCR) was performed to evaluate the expression levels of target genes. The RT-qPCR analyses were conducted using CXCR4-specific primers (F: 5′-CTC CTC TTT GTC ATC ACG CTT CC-3′, R: 5′-GGA TGA GGA CAC TGC TGT AGA G-3′) along with 800 ng of template DNA and 2X QGreenBlue qPCR Master Mix (CellSafe, Seoul, Korea). The components were mixed together and then subjected to thermal cycling using a Bio-Rad thermal cycler (CA, USA). The thermal cycling

protocol included a pre-denaturation step at 95 °C for 3 min, followed by 40 cycles of denaturation at 95 °C for 10 s, annealing at 58 °C for 10 s, extension and fluorescence detection at 72 °C for 10 s, and a final melting curve analysis step. The RT-qPCR data obtained was then utilized to calculate the relative expression levels of the target genes using the $2-\Delta\Delta Ct$ method. GAPDH was used as a reference gene.

2.6. Protein extraction and western blotting

The MIO-M1 cells were first lysed for protein extraction and isolation in RIPA lysis buffer containing protease and phosphatase inhibitors (ATTO; Tokyo, Japan). The lysates were then centrifuged at $13,000 \times g$ for 20 min at 4 °C. The resulting protein-enriched supernatant was collected and protein concentration was analyzed using the Pierce BCA Protein Assay Kit (Thermo Fisher Scientific, Inc., MA, USA). The expression of the proteins was validated through western blot analysis.

To determine the protein expression levels in MIO-M1 cells, total protein extracts were subjected to 12 % sodium dodecyl sulfate-polyacrylamide gel electrophoresis (SDS-PAGE) with 20 μg of total proteins per lane. The separated proteins were then transferred onto polyvinylidene fluoride (PVDF) membranes through a semi-dry blotting procedure (ATTO) at a 500 mA current for 20 min. The PVDF membranes were blocked with 5 % skim milk (v/v) to minimize non-specific binding before incubating overnight with the relevant primary antibodies (as listed in Additional file 1: Table S1) at 4 °C. After washing the samples three times with Tris-buffered saline with 0.1 % Tween 20 (TTBS), the PVDF membranes were incubated with horseradish peroxidase (HRP)-conjugated secondary antibodies for 1 h at room temperature. Next, a RIPA lysis buffer containing a protease and phosphatase inhibitor cocktail (ATTO) was used to isolate the proteins from MIO-M1 cells. The protein expression levels were then determined through western blotting using a ChemiDoc XRS + system and the signals were quantified using the ImageJ software (National Institutes of Health; MD, USA).

2.7. Cytokine/chemokine protein profiling array

A total of 40 cytokine and chemokine proteins were analyzed in each protein sample (100 μL) using the Cytokine Protein Proteomic Profiler™ Array kit (R&D Systems, MN, USA) according to the manufacturer's instructions. The pixel densities of the resulting western blotting dots were quantified using ImageJ, and two measurements were taken from each sample, with the duplicate spots being averaged to obtain the final value.

2.8. Zebrafish histology analysis

Adult zebrafish were fixed with 10 % NBF for 1 d at 4 °C. Following fixation, the zebrafish were rinsed with distilled water. The paraffin-embedded tissues were processed using a tissue processor (Thermo Fisher Scientific; MA, USA) and sliced to 4 μm thick sections.

Hematoxylin & Eosin (H&E) staining is a widely used method in histology that allows for the visualization of different cellular and tissue structures under a light microscope. The paraffin-embedded sections were immersed in 100 % xylene to remove the paraffin, then subjected to a series of increasing ethanol concentrations. After washing with water, the slides were stained with hematoxylin, which stains the nuclei blue, for 1 min. The slides were then stained with eosin, a red-pink dye that binds to the essential components of tissue, including the cytoplasm, extracellular matrix, and other organelles. Finally, the slides were mounted with glycerol on a microscope slide and covered with a coverslip before being examined under a light microscope (Olympus Optical Co.).

2.9. Immunohistochemistry

The de-paraffinized tissue slides were incubated with 0.3 % hydrogen peroxide solution (Merk; MO, USA) for 10 min. The slides were then rinsed with PBS and incubated with normal animal serum from an ABC kit for 1 h at room temperature. Afterward, the slides were incubated with anti-CXCL12 primary antibodies for 1 d at 4 °C and rinsed thrice with PBS. The tissue slides were then incubated with biotinylated goat anti-rabbit IgG secondary antibodies and incubated with an avidin-biotin complex from the ABC kit. The tissue slides were developed with DAB (Sigma-Aldrich) as a substrate for 5 min, mounted with a xylene-based DPX solution (Sigma-Aldrich), and visualized via light microscopy (Olympus Optical Co.).

2.10. Terminal deoxynucleotidyl transferase dUTP nick end labeling (TUNEL) assay

A terminal deoxynucleotidyl transferase dUTP nick end labeling (TUNEL) assay was performed to detect apoptotic cell death in zebrafish tissue. First, we de-paraffinized the tissue slides and then immersed them in PBS for 5 min. Next, the slides were permeabilized on ice with freshly prepared 0.1 % Triton X-100 in PBS for 10 min. After rinsing the slides twice with PBS, the TUNEL reaction mixture (Hoffman-La Roche Ltd.) was added to the tissue slides, after which the samples were incubated at 37 °C in a humidified atmosphere in the dark for 60 min. After another rinse with PBS, the slides were incubated with 1 μg/mL 4′,6-diamino-2-phenylindole (Sigma-Aldrich) for 30 s. Finally, the tissue slides were mounted using Vectashield mounting media (Vector Laboratories) and imaged using an LSM 710 confocal microscope (Carl Zeiss, Göttingen, Germany).

2.11. Statistical analysis

The data analysis was performed using GraphPad Prism 6 software. One-way analysis of variance (ANOVA) was conducted, followed by Tukey's test for multiple comparisons. A significance level of $P < 0.05$ was used to determine statistical significance. When employing letter annotations to indicate statistical differences, groups marked with the same letter did not exhibit any significant difference, while significant differences were observed between any two groups marked with different letters.

3. Results

3.1. Establishment of BL-exposed retinal phototoxicity models and the role of DPHC in modulating CXCR4 expression

First, we prepared a BL device to establish a BL-induced retinal phototoxicity model. The device consisted of six BL-emitting diode (LED; 390–410 nm) modules mounted on a metal printed circuit board (PCB) and six heat sinks to decrease heat damage (Supplementary Fig. S1). Next, MIO-MI cells were kept in the dark (dark group) or under BL exposure (BL group) for 100 min. Some MIO-M1 cells were treated with DPHC (5 μM or 10 μM) for 1 day prior to BL exposure (BL/DPHC group) (Fig. 1A). After BL exposure, the expression level of C-X-C motif chemokine 12 (CXCL12, red box) increased compared to the dark group. In contrast, CXCL12 expression decreased in the 10 μM DPHC-treated cells (Fig. 1B and C). Interestingly, the protein and mRNA levels of CXCR4, the receptor of CXCL12, also increased in the BL-exposed group compared to the dark group. However, DPHC treatment reduced these expression levels compared to the BL group (Fig. 1D–F). These results confirm that our BL-exposed retinal phototoxicity model
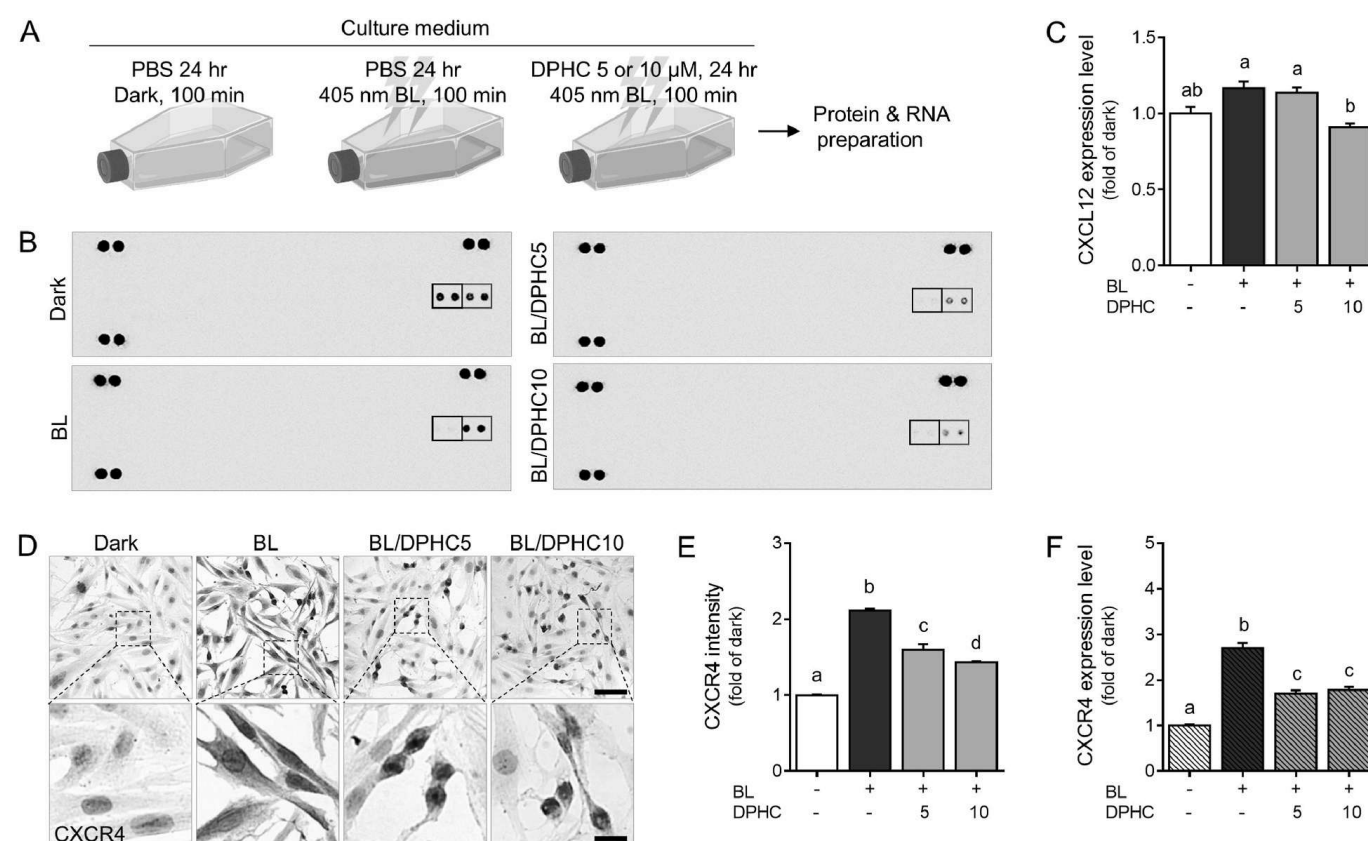
Fig. 1. *In vitro* modeling of the effect of BL exposure on CXCL12 and CXCR4 expression (A) Schematic image showing the establishment of an in vitro model of BL damage using a BL LED device. Figure (A) generated with BioRender (https://biorender.com/). (B) After a 100 min of BL exposure, a cytokine array analysis was conducted. The protein expression of chemokine (C-C motif) ligand 5 (also known as CCL5) (indicated by the black box) decreased in the BL group compared to the dark group, but there were no changes in the BL/DPHC groups. (B, C) Conversely, CXCL12 protein expression (indicated by the red box) increased only in the MIO-M1 cell group exposed to BL (BL group) compared to the MIO-M1 cells exposed to darkness (Dark group). However, the CXCL12 protein expression decreased in the DPHC-treated BL-exposed MIO-M1 cell group (the BL/DPHC groups) compared to the BL group. (D–F) BL exposure increased (D, E) the protein expression of CXCR4, which is the receptor of CXCL12, compared to the dark group. Interestingly, (F) the CXCR4 mRNA expression followed a similar pattern to the protein expression. DPHC treatment decreased both the protein and mRNA expression of CXCR4. The results presented in this study are expressed as the mean ± SEM. One-way ANOVA was conducted, followed by Tukey's multiple comparisons test ($p < 0.05$). Distinct letters (a, b, c, d) above the bars denote groups that differ significantly ($p < 0.05$), while bars sharing the same letter are not significantly different. Each experiment was performed at least three times independently. Scale bar = 100 μm, BL, blue light; CCL5, chemokine (C-C motif) ligand 5; CXCL12, C-X-C motif chemokine ligand 12; CXCR4, C-X-C chemokine receptor type 4; DPHC, diphlorethohydroxycarmalol.
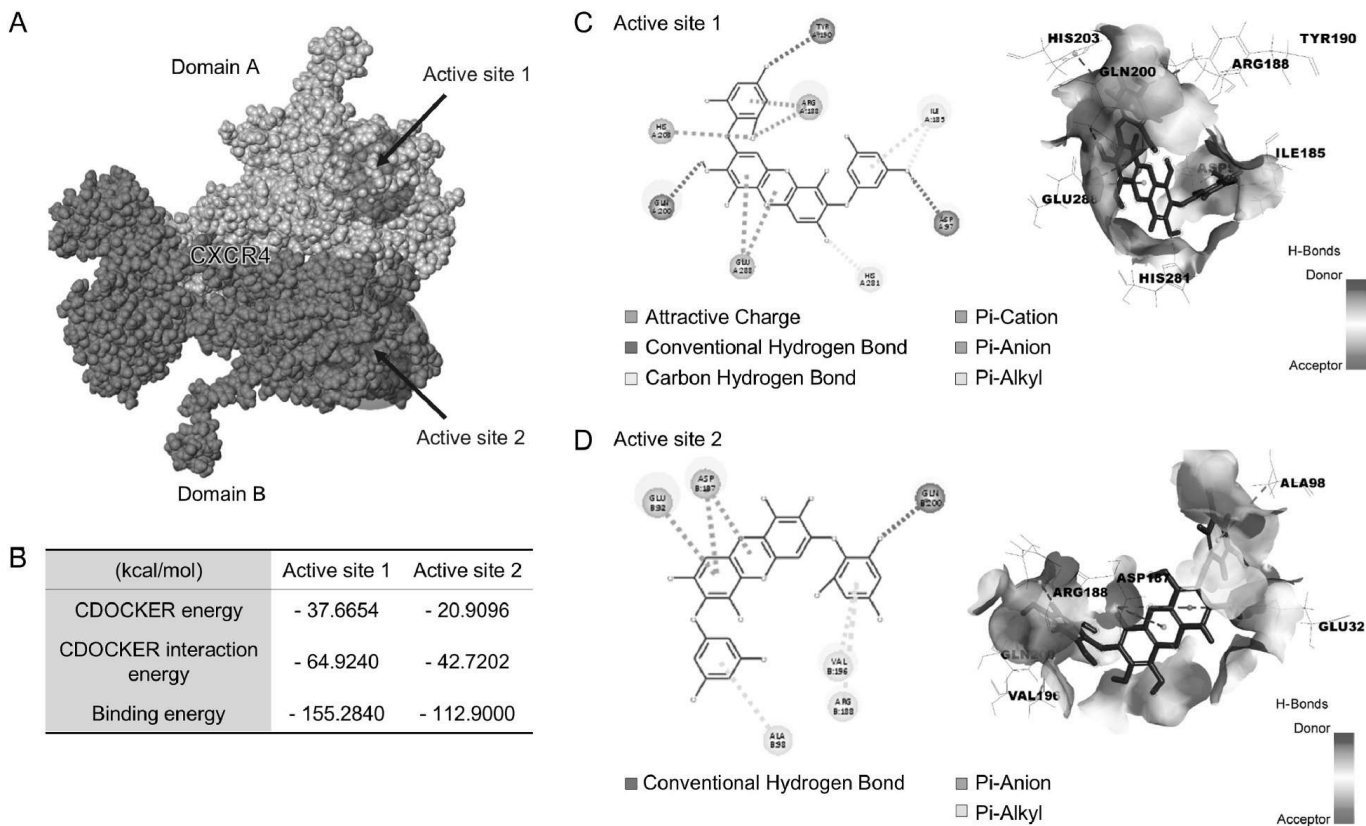
successfully induces CXCL12 and CXCR4 upregulation as well as demonstrate that pre-treatment with DPHC effectively counteracts this increase, thereby potentially mitigating early inflammatory and gliotic responses.

3.2. Analysis of CXCR4-DPHC interaction and binding affinity through computational predictions

Fig. 2 illustrates the computational predictions of the CXCR4 structure. The identification of the active sites 1 and 2 of CXCR4 within domains A and B, respectively, is illustrated in Fig. 2A. The analysis of the binding affinity between DPHC and the two active sites of CXCR4 revealed that site 1 exhibited a stronger interaction, with a binding energy of −155.2840 kcal/mol, compared to site 2, which had a binding energy of −112.9000 kcal/mol. The CDOCKER energy values of CXCR4-DPHC were determined to be −37.6654 kcal/mol and −20.9096 kcal/mol for sites 1 and 2, respectively (Fig. 2B). The interaction between DPHC and CXCR4 was further investigated by analyzing three conventional hydrogen bonds formed between DPHC and ASP97, TYR190, and GLN200, as well as two carbon-hydrogen bonds formed between DPHC and ILE185 and HIS281, and three weaker bonds between DPHC and ARG188, HIS208, and GLU288 in domain A (Fig. 2C). Additionally, the stability of DPHC at active site 2 was found to be supported through one conventional hydrogen bond with GLN200 and two pi-anion bonds with GLU92 and ASP187, as well as three pi-alkyl bonds with ALA98, ARG188, and VAL196 in domain B (Fig. 2D). Overall, these computational predictions confirm a strong and specific interaction between DPHC and the primary CXCR4 active site, highlighting key binding residues and providing a molecular basis for DPHC's potential to modulate CXCR4-mediated pathways.

### 3.3. Inhibition of Müller gliosis induced by DPHC treatment with BL damage in vitro

Fig. 2 demonstrates that DPHC can bind to active site 1 of CXCR4, leading to the inhibition of BL-induced Müller gliosis. Müller gliosis is a well-known response to retinal injury, including BL exposure [23]. In this study, we evaluated the inhibitory effects of DPHC on BL-exposed MIO-M1 cells by assessing the expression of glial fibrillary acidic protein (GFAP) and glutamine synthetase (GS), both of which are markers of Müller gliosis. The expression of the GFAP protein was significantly higher in the BL group than in the dark group. However, treatment with 10 μM DPHC reduced GFAP expression even under BL damage (Fig. 3A and B). Similarly, the expression of GS was altered in the BL group compared to the dark group, whereas DPHC treatment restored GS expression even under BL damage (Fig. 3C). A recent study reported that gliosis leads to swelling of the Müller glial cell body or soma [23]. Consistent with these findings, we observed that BL exposure caused an increase in the soma area compared to the dark group, whereas DPHC treatment reduced the

(kcal/mol)	Active site 1	Active site 2
CDOCKER energy	- 37.6654	- 20.9096
CDOCKER interaction energy	- 64.9240	- 42.7202
Binding energy	- 155.2840	- 112.9000

Fig. 2. Diphlorethohydroxycarmalol (DPHC) as a CXCR4 binding inhibitor (A) 3D computational predictions of the CXCR4 structure, with two domains containing two active sites. (B) The table displays the CDOCKER energy, interaction energy (at active site 1/CXCR4 and active site 2/ CXCR4), and binding energy. (C, D) 2D computational predictions of the CXCR4 structure shown as conventional hydrogen bonds. CXCR4, C-X-C chemokine receptor type 4.

soma area even under BL exposure (Fig. 3D and E). Therefore, these results suggest that DPHC treatment can effectively inhibit Müller gliosis in response to BL-exposed retinal damage. Our study found that exposure to BL leads to increased expression of CXCR4 and its ligand, CXCL12 (Fig. 1). This upregulation subsequently triggers Müller gliosis in vitro (Fig. 3A–C). To further investigate the direct induction of Müller gliosis by CXCL12, we established a CXCL12-induced MIO-M1 cell model. Prior to treatment with 20 nM CXCL12 for 24 h, MIO-M1 cells were subjected to 5 and 10 μM DPHC treatment (Fig. 3F). Our results showed that CXCL12 caused alterations in the expression of gliosis markers, specifically GFAP and GS. However, DPHC treatment restored the protein expression levels of GFAP and GS (Fig. 3G–I).

It is worth noting that nuclear factor kappa-light-chain-enhancer of activated B cells (NF-κB) signaling is known to promote glial
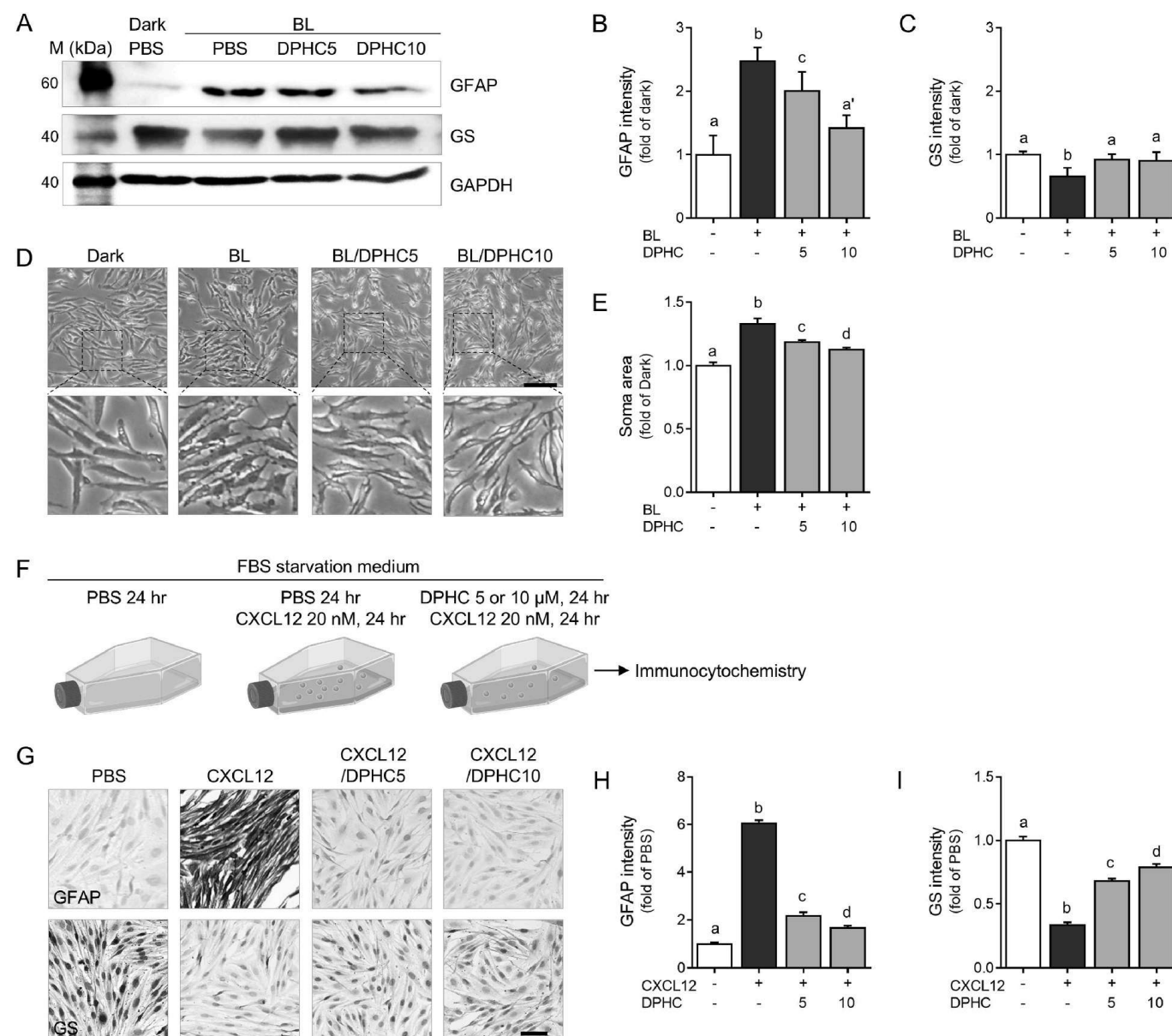

Fig. 3. Validation of reactive Müller glia markers in DPHC-treated MIO-M1 cells after BL damage or CXCL12 induction (A) To validate the reactive Müller glia marker expression in MIO-M1 cells, GFAP and GS protein expression was characterized using western blot analysis after BL exposure. Standard protein markers were loaded in the far left lane. The uncropped and non-adjusted images can be found in the supplementary Fig. 2 (B, C) The graphs show the expression intensity of GFAP and GS after BL damage. (D) The cell images demonstrate changes in cell morphology after BL damage. Scale bar = 200 μm (E) BL damage altered the soma area or cell body. (F) Schematic image showing the establishment of an in vitro model of CXCL12 induction. Figure (F) generated with BioRender (https://biorender.com/). (G–I) To validate the reactive Müller glia marker expression in CXCL12 induced MIO-M1 cells, GFAP and GS protein expression was characterized using immunocytochemistry. Scale bar = 100 μm (H, I) The quantified graphs show GFAP and GS expression levels after CXCL12 induction. The results presented in this study are expressed as the mean ± SEM. One-way ANOVA was conducted, followed by Tukey's multiple comparisons test ($p < 0.05$). Distinct letters (a, b, c, d) above the bars denote groups that differ significantly ($p < 0.05$), while bars sharing the same letter are not significantly different. Each experiment was performed at least three times independently. Scale bar = 100 μm, BL, blue light; DPHC, diphlorethohydroxycarmalol; GAPDH, glyceraldehyde 3-phosphate dehydrogenase; GFAP, glial fibrillary acidic protein; GS, glutamine synthetase.

reactivity [24]. Therefore, to examine the involvement of CXCR4-NF-κB signaling, we analyzed the expression of these molecules (Fig. 4A). Gliosis is characterized by increased proliferation and glial reactivity, which are associated with ERK and AKT phosphorylation, respectively (Fig. 4B–D). Importantly, we found that NF-κB phosphorylation was elevated in the BL-exposed group compared to the dark group. At the same time, DPHC treatment decreased NF-κB expression and ERK and AKT phosphorylation (Fig. 4B–E). To summarize, these experiments demonstrate that DPHC treatment effectively inhibits Müller gliosis triggered by BL exposure and CXCL12 stimulation, likely through the suppression of CXCR4-NF-κB signaling and subsequent modulation of ERK and AKT pathways, ultimately preserving the homeostatic functions of Müller cells under phototoxic stress.

3.4. Inhibition of BL-induced Müller gliosis and cell death by DPHC treatment in vivo

In this study, we confirmed the inhibitory effects of DPHC on Müller gliosis in vitro. To further investigate this effect *in vivo*, we established an *in vivo* zebrafish model of BL damage (Fig. 5A). The retina is a complex tissue consisting of various cell types including the retinal pigment epithelium, photoreceptors, horizontal cells, bipolar cells, and ganglion cells. Among them, bipolar cells are critical in transmitting visual stimuli. For instance, the high sensitivity of the foveal region can be attributed to the arrangement of photoreceptors and bipolar cells. The outer nuclear layer (ONL) contains photoreceptors, whereas the inner nuclear layer (INL) contains horizontal cells, bipolar cells, amacrine cells, and Müller cells [25]. Here, H&E staining was used to examine the histological features of the retina.

Our results demonstrated that zebrafish with BL damage had a significantly decreased retinal thickness compared to the dark group. However, DPHC treatment effectively restored the retinal thickness even in the presence of BL damage (Fig. 5B and C). Furthermore, we observed an increase in CXCL12 protein expression in the INL of the BL group compared to the dark group. Nevertheless, treatment with 10 μM DPHC decreased CXCL12 expression even in the presence of BL damage (Fig. 5D). Finally, TUNEL staining revealed a significant increase in the number of apoptotic cells in both the ONL and INL of the BL-damaged group compared to the dark group. However, treatment with 5 and 10 μM DPHC reduced the number of apoptotic cells even in the presence of BL damage (Fig. 5E and F). In summary, these animal study findings further reinforce the protective role of DPHC in mitigating BL-induced Müller gliosis and retinal cell death, highlighting its potential to preserve retinal integrity and cellular viability under phototoxic conditions.
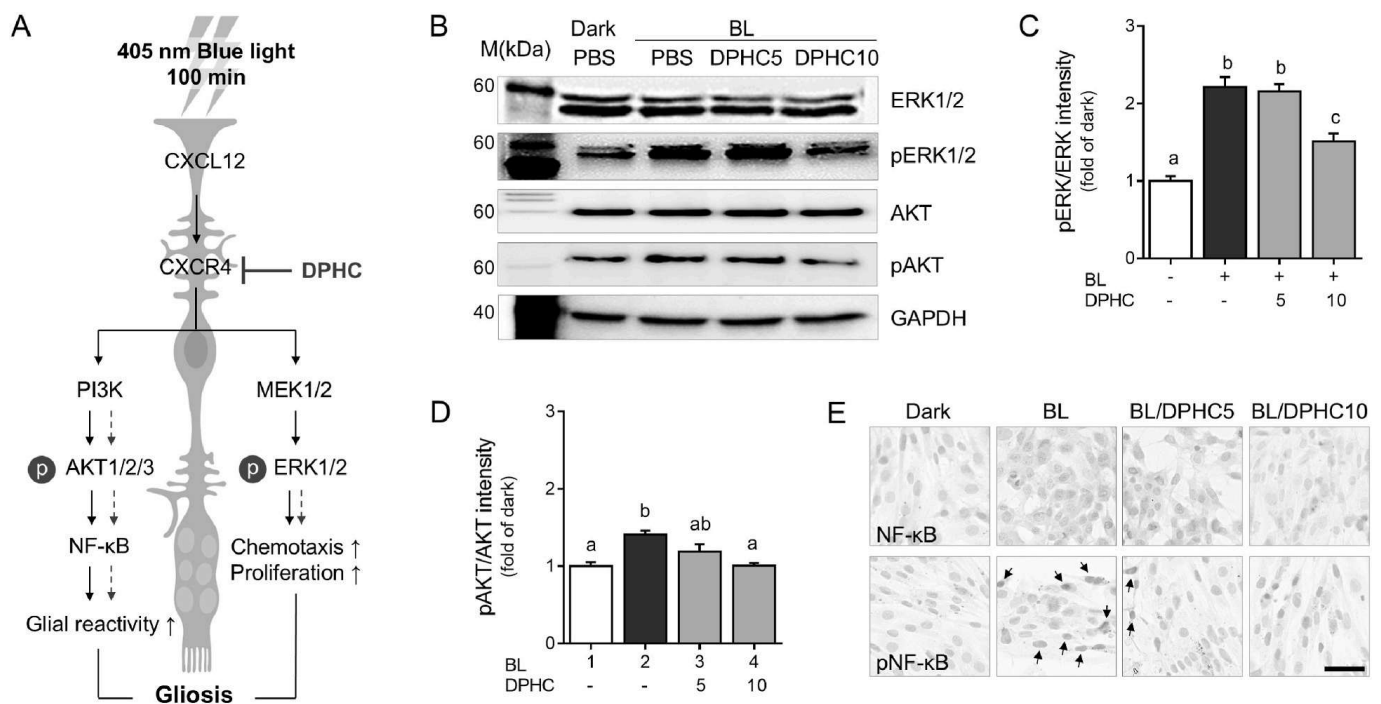
Fig. 4. Validation of CXCR4-NF-κB signaling in DPHC-treated MIO-M1 cells after BL damage (A) Schematic depiction of the role of CXCR4-NF-κB signaling in glial gliosis. In DPHC-treated MIO-M1 cells, DPHC tends to bind to CXCR4 instead of its ligand CXCL12. Figure (A) generated with BioRender (https://biorender.com/). (B–D) (B) The results of western blot analysis and protein expression quantification revealed that DPHC treatment resulted in altered phosphorylation of (C) ERK1/2 (Thr183/Tyr 185), (D) AKT1/2/3 (Thr 308/Ser 473). The uncropped and non-adjusted images can be found in the Supplementary Fig. 3. (E) The translocation of pNF-κB from the cytoplasm to the nucleus was validated using immunocytochemistry. Arrows indicate expression of pNF-κB in nucleus of MIO-M1 cells. Scale bar = 50 μm Standard protein markers were loaded in the far left lane. The results presented in this study are expressed as the mean ± SEM. One-way ANOVA was conducted, followed by Tukey's multiple comparisons test (p < 0.05). Distinct letters (a, b, c, d) above the bars denote groups that differ significantly (p < 0.05), while bars sharing the same letter are not significantly different. Each experiment was performed at least three times independently. AKT1/2/3, Akt serine/threonine kinase family 1/2/3; BL, blue light; DPHC, diphlorethohydroxycarmalol; ERK1/2, extracellular signal-regulated kinase 1/2; GAPDH, glyceraldehyde 3-phosphate dehydrogenase; NF-κB, nuclear factor kappa-light-chain-enhancer of activated B cells.
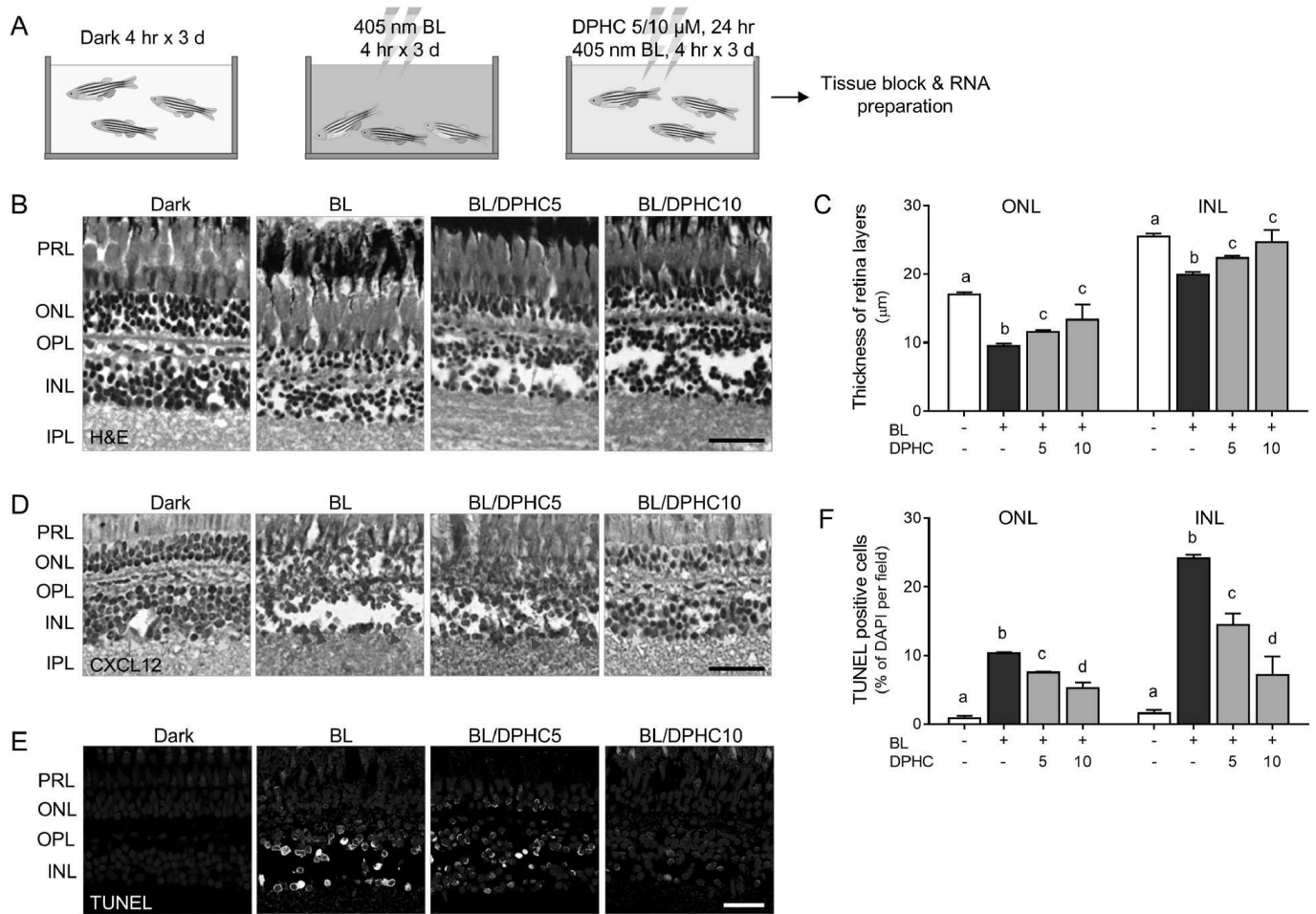
Fig. 5. Inhibitory effects of DPHC on Müller gliosis of zebrafish eyes after BL damage (A) Schematic illustrating the role of DPHC in the development of gliosis in zebrafish. To induce retinal gliosis, zebrafish were exposed to BL for 4 h per day over a 3 d period. Figure (A) generated with BioRender (https://biorender.com/). (B, C) Histological changes in the zebrafish retina were assessed through H&E staining, and the thickness of the retina was measured using the ImageJ software. (D) The red arrowheads indicate CXCL12 expression in the cells, whereas the yellow arrowheads indicate the absence of CXCL12 staining. (E, F) TUNEL staining, which detects apoptotic retinal cells, was used to stain the positive cells (white), whereas DAPI stained the nucleus in blue. The TUNEL-positive cells (white) were counted using the ImageJ software and the graph represents the quantification of apoptotic cell numbers derived from representative images. The results presented in this study are expressed as the mean ± SEM. One-way ANOVA was conducted, followed by Tukey's multiple comparisons test ($p < 0.05$). One-way ANOVA was conducted, followed by Tukey's multiple comparisons test ($p < 0.05$). Distinct letters (a, b, c, d) above the bars denote groups that differ significantly ($p < 0.05$), while bars sharing the same letter are not significantly different. Each experiment was performed at least three times independently. Scale bar = 20 μm, BL, blue light; CXCL12, C-X-C motif chemokine ligand 12; DAPI, 4′,6-diamidino-2-phenylindole; DPHC, diphlorethohydroxycarmalol; H&E, hematoxylin & eosin, INL, inner nuclear layer; IPL, inner plexiform layer; ONL, outer nuclear layer; OPL, outer plexiform layer; PRL, photoreceptor layer; TUNEL, terminal deoxynucleotidyl transferase dUTP nick end labeling.

4. Discussion

CXCL12 is a natural ligand for CXCR4 that plays a crucial role in recruiting and activating various cell types in the retina, including glial cells. The expression of CXCL14 in different ocular tissues, along with the expression of CXCL12 in the periocular mesenchyme, ocular blood vessels, retina, and eyelid mesenchyme, suggests that these two chemokines may interact and contribute to cell proliferation, differentiation, and migration during eye development in chick and mouse retinas [26]. However, CXCL12 has also been found to induce neurotoxicity in cerebrocortical neurons, although the cellular mechanisms underlying this effect are not fully understood. Additionally, The co-receptor CXCR4 mediates the neurotoxicity of the viral envelope protein gp120 and is also involved in human immunodeficiency virus (HIV)-1 infection [27]. Our study demonstrates that DPHC inhibits Müller cell gliosis by disrupting the CXCR4/CXCL12 interaction, leading to the attenuation of downstream ERK and AKT signaling pathways (Figs. 2 and 4). This indicates a novel mechanism of action for DPHC, distinct from its previously reported interactions with TNF-α. While TNF-α is a critical mediator of inflammation, our results suggest that targeting the CXCR4/CXCL12 axis may offer additional therapeutic benefits.

Overexposure to BL has been associated with various adverse effects, such as retinal damage, insomnia, and vision impairment. It can also prompt photoreceptor death and retinal gliosis, which are linked to several retinal diseases. However, there is no conclusive evidence that long-term exposure to blue light at lower intensities causes damage to the retina in humans. Despite this, it is important

to note that Müller gliosis, a form of glial cell activation, has been observed in response to overexposure to BL and can result in retinal degeneration [28–31]. This study explored the relationship between CXCL12 expression and Müller gliosis in response to BL damage. The BL damage induced an increase in the expression of CXCL12 and that of its receptor, CXCR4, in MIO-M1 cells (Fig. 1).

Phenotypic changes in glial cells, including cellular hypertrophy and increased GFAP expression, are often associated with Müller gliosis [32]. In this study, BL damage induced Müller gliosis in MIO-M1 cells. GFAP and GS are representative markers of Müller gliosis and their expression levels were altered after BL damage in MIO-M1 cells (Fig. 3). One study demonstrates that MIO-M1 cells exposed to high glucose (25 mM) and hydrogen peroxide (H_2O_2) exhibit lower GS levels and increased migration capacity compared to MIO-M1 cells exposed to PBS. Additionally, the combination of high glucose and oxidative stress in MIO-M1 cells can significantly impact the reprogramming capacity of Müller cells [33]. Additionally, NF-κB signaling is essential in the gliosis process. A previous study explored the role of NF-κB signaling in RMGs after retinal damage. The study demonstrated that retinal damage activates NF-κB and associated genes in RMGs, and inhibiting NF-κB increases the reprogramming of RMGs into neuron-like cells. The inhibition of Smad3 or Id transcription factors also increases neuron-like cells. The authors thus concluded that NF-κB is crucial in mediating the accumulation of immune cells and suppressing the neurogenic potential of RMGs [24]. Another study investigated the role of NF-κB signaling in the suppression of retinal regeneration in warm-blooded vertebrates. The study used a chick *in vivo* model and inhibiting NF-κB was found to enhance the formation of proliferating Müller glia-derived progenitor cells (MGPCs), whereas activation suppresses their formation. This study suggested that NF-κB is a vital signaling hub that suppresses the reprogramming of Müller glia into MGPCs and that reactive microglia influences NF-κB-mediated Müller glia reprogramming [34].

Importantly, our results also show that BL-induced upregulation of ERK and AKT in Müller cells is attenuated by DPHC treatment (Fig. 4). Both ERK and AKT pathways play critical roles in gliosis and cell survival; ERK activation can contribute to autophagy regulation and energy metabolism by upregulating GLUT1, while AKT can prevent apoptosis by activating mTOR and other downstream targets [35]. By downregulating these key pathways, DPHC likely mitigates the oxidative stress and inflammatory responses that drive Müller gliosis. This highlights how DPHC's suppression of ERK and AKT phosphorylation complements its disruption of the CXCR4/CXCL12 axis, effectively reducing glial reactivity and alleviating the gliosis-promoting environment in the retina. Furthermore, NF-κB activation, also play significant roles in gliotic responses, is a key driver of inflammation and immune cell recruitment in the retina following injury. However, its inhibition has been shown to suppress gliotic responses and enhance the reprogramming of Müller glia into neuron-like cells, mediated through its interplay with TGFβ2 signaling and suppression of pro-gliotic transcription factors like Smad3 proteins [36].

In our study, DPHC treatment not only reduced NF-κB expression but also inhibited the phosphorylation of ERK and AKT signaling. These findings suggest that DPHC mitigates gliosis by targeting multiple pathways involved in stress and immune signaling, thus creating an environment less conducive to glial reactivity and inflammation. Our findings highlight the multifaceted mechanisms by which DPHC exerts its protective effects on Müller cells under BL-induced stress. Beyond disrupting the CXCR4/CXCL12 axis, DPHC's simultaneous inhibition of ERK, AKT, and NF-κB pathways emphasizes its potential as a therapeutic agent for retinal disorders characterized by gliosis and chronic inflammation.

Some single compounds from natural sources show suppression of Müller gliosis. For instance, resveratrol, a naturally occurring antioxidant found in red grapes, has been found to have protective effects against streptozotocin (STZ)-induced apoptosis of the INL in the retinal layer [37]. Curcumin, a phytocompound derived from turmeric, has also been investigated as a promising therapeutic agent for the treatment and prevention of retinal diseases, including Müller cell activation and diabetic retinal oxidative stress [38]. In this study, we examined the potential therapeutic effects of DPHC treatment at 5 or 10 μM in both in vitro and *in vivo* models of BL-exposed damage. Bioactive compounds have diverse functional activities influenced by their unique structural characteristics, including hydrophobicity, charge, and microelement binding capacity. Our findings indicated that DPHC treatment effectively suppresses glial reactivity and prevents retinal neuron apoptosis, as demonstrated in Figs. 3 and 5. Although no previous studies have investigated the role of DPHC in the retina, it has been reported to inhibit the expression of pro-inflammatory cytokines and matrix metalloproteinases (MMPs) in UVB-irradiated human dermal fibroblasts [37]. Furthermore, DPHC also exerts protective effects against *in vivo* photodamage in UVB-irradiated zebrafish by decreasing reactive oxygen species (ROS) levels and reducing lipid peroxidation and inflammation, thereby decreasing cell death [39]. The notion that polyphenols, including DPHC, protect cells by scavenging free radicals is an oversimplified view. Their biological effects extend beyond oxidative stress modulation [40,41].

Over the past decades, the zebrafish has emerged as a valuable model organism for investigating various aspects of eye diseases. Particularly, zebrafish have been widely utilized in ophthalmology research due to their well-characterized developmental processes and the availability of zebrafish lines with natural mutations [42]. In this study, we aimed to establish a zebrafish model to confirm the inhibitory effects of DPHC on BL-induced retinal damage (Fig. 5). Unlike mammals, teleost fish such as zebrafish can regenerate retinal neurons to replace those lost due to injury or disease [43,44]. The retina of a lesioned zebrafish can regenerate neurons of all types from the same lineage that produces only rods. RMG-derived progenitors for margin neurons, rod photoreceptors, and regenerated neurons originate from multipotent stem cells, which are associated with growth-related neurogenic activity. Therefore, future studies must investigate the relationship between DPHC, RMG-derived progenitors, and major retinal neurons. In conclusion, our findings indicated that DPHC derived from brown seaweeds is a promising bioactive compound for the treatment of retinal diseases related to Müller gliosis. However, additional research, including animal studies and human clinical trials, is needed to gain more insights into their potential as therapeutic agents.

5. Conclusion

In summary, this study demonstrates the potential of DPHC, a natural bioactive compound derived from *Ishige okamurae,* to inhibit

Müller gliosis, a crucial process for retinal health and function. The study provides evidence that DPHC suppresses Müller gliosis by downregulating the ERK/AKT/NF-κB pathway through CXCR4 inhibition, resulting in altered expression of Müller gliosis markers and reduced retinal cell apoptosis. These findings indicate that DPHC can potentially be a promising therapeutic agent for retinal diseases involving Müller gliosis. Moreover, this study highlights the potential of natural bioactive compounds as sources of therapeutic agents for various diseases. Future studies should investigate the full therapeutic potential of DPHC and its derivatives in treating retinal diseases.

CRediT authorship contribution statement

Myeongjoo Son: Writing – original draft, Funding acquisition, Formal analysis, Data curation. **Dineth Pramuditha Nagahawatta:** Visualization, Resources. **Hang-Chan Jo:** Visualization, Resources. **You-Jin Jeon:** Resources, Conceptualization. **Bomi Ryu:** Writing – original draft, Data curation. **Dae Yu Kim:** Writing – original draft, Methodology, Funding acquisition.

Data availability statement

Data will be made available on request (dyukim@inha.ac.kr, D.Y. Kim; mjson@kangwon.ac.kr, M. Son).

Ethics declaration

All zebrafish experiments complied with the ethical guidelines set by the Experimental Animal Ethical Committee under the Institutional Animal Care and Use Committee (IACUC) at Inha University. The study was approved under protocol number INHA 221121-844.

Declaration of competing interest

The authors declare that they have no known competing financial interests or personal relationships that could have appeared to influence the work reported in this paper.

Acknowledgment

Appendix A. Supplementary data

Supplementary data to this article can be found online at https://doi.org/10.1016/j.heliyon.2025.e42475.

References

[1] R. Wang, H. Ren, Y. Gao, G. Wang, Editorial: role of glial cells of the central and peripheral nervous system in the pathogenesis of neurodegenerative disorders, Front. Aging Neurosci. 14 (2022) 920861, https://doi.org/10.3389/fnagi.2022.920861.

[2] A. Bringmann, T. Pannicke, J. Grosche, M. Francke, P. Wiedemann, S.N. Skatchkov, N.N. Osborne, A. Reichenbach, Müller cells in the healthy and diseased retina, Prog. Retin. Eye Res. 25 (2006) 397–424, https://doi.org/10.1016/j.preteyeres.2006.05.003.

[3] A. Bringmann, I. Iandiev, T. Pannicke, A. Wurm, M. Hollborn, P. Wiedemann, N.N. Osborne, A. Reichenbach, Cellular signaling and factors involved in Müller cell gliosis: neuroprotective and detrimental effects, Prog. Retin. Eye Res. 28 (2009) 423–451, https://doi.org/10.1016/j.preteyeres.2009.07.001.

[4] R. Afridi, M. Tsuda, H. Ryu, K. Suk, The function of glial cells in the neuroinflammatory and neuroimmunological responses, Cells 11 (2022) 659, https://doi.org/10.3390/cells11040659.

[5] B.V. Fausett, D. Goldman, A role for alpha1 tubulin-expressing Müller glia in regeneration of the injured zebrafish retina, J. Neurosci. 26 (2006) 6303–6313, https://doi.org/10.1523/jneurosci.0332-06.2006.

[6] B.V. Fausett, J.D. Gumerson, D. Goldman, The proneural basic helix-loop-helix gene ascl1a is required for retina regeneration, J. Neurosci. 28 (2008) 1109–1117, https://doi.org/10.1523/jneurosci.4853-07.2008.

[7] S. Wahl, M. Engelhardt, P. Schaupp, C. Lappe, I.V. Ivanov, The inner clock-Blue light sets the human rhythm, J. Biophot. 12 (2019) e201900102, https://doi.org/10.1002/jbio.201900102.

[8] E.E. Flynn-Evans, L.K. Barger, A.A. Kubey, J.P. Sullivan, C.A. Czeisler, Circadian misalignment affects sleep and medication use before and during spaceflight, NPJ Microgravity 2 (2016) 15019, https://doi.org/10.1038/npjmgrav.2015.19.

[9] J. Kim, K. Cho, S.Y. Choung, Protective effect of Prunella vulgaris var. L extract against blue light induced damages in ARPE-19 cells and mouse retina, Free Radic. Biol. Med. 152 (2020) 622–631, https://doi.org/10.1016/j.freeradbiomed.2019.12.003.

[10] M. Marie, K. Bigot, C. Angebault, C. Barrau, P. Gondouin, D. Pagan, S. Fouquet, T. Villette, J.A. Sahel, G. Lenaers, S. Picaud, Light action spectrum on oxidative stress and mitochondrial damage in A2E-loaded retinal pigment epithelium cells, Cell Death Dis. 9 (2018) 287, https://doi.org/10.1038/s41419-018-0331-5.

[11] A. Bringmann, P. Wiedemann, Müller glial cells in retinal disease, Ophthalmologica 227 (2012) 1–19, https://doi.org/10.1159/000328979.

[12] I. Iandiev, A. Wurm, M. Hollborn, P. Wiedemann, C. Grimm, C.E. Remé, A. Reichenbach, T. Pannicke, A. Bringmann, Müller cell response to blue light injury of the rat retina, Investig. Ophthalmol. Vis. Sci. 49 (2008) 3559–3567, https://doi.org/10.1167/iovs.08-1723.

[13] A. Bringmann, T. Pannicke, J. Grosche, M. Francke, P. Wiedemann, S.N. Skatchkov, N.N. Osborne, A. Reichenbach, Müller cells in the healthy and diseased retina, Prog. Retin. Eye Res. 25 (2006) 397–424, https://doi.org/10.1016/j.preteyeres.2006.05.003.

[14] R. Janssens, S. Struyf, P. Proost, The unique structural and functional features of CXCL12, Cell. Mol. Immunol. 15 (2018) 299–311, https://doi.org/10.1038/cmi.2017.107.

[15] A. Guyon, CXCL12 chemokine and its receptors as major players in the interactions between immune and nervous systems, Front. Cell. Neurosci. 8 (2014) 65, https://doi.org/10.3389/fncel.2014.00065.

[16] X.Q. Li, Z.L. Zhang, W.F. Tan, X.J. Sun, H. Ma, Down-regulation of CXCL12/CXCR4 expression alleviates ischemia-reperfusion-induced inflammatory pain via inhibiting glial TLR4 activation in the spinal cord, PLoS One 11 (2016) e0163807, https://doi.org/10.1371/journal.pone.0163807.

[17] R. Bonavia, A. Bajetto, S. Barbero, P. Pirani, T. Florio, G. Schettini, Chemokines and their receptors in the CNS: expression of CXCL12/SDF-1 and CXCR4 and their role in astrocyte proliferation, Toxicol. Lett. 139 (2003) 181–189, https://doi.org/10.1016/s0378-4274(02)00432-0.

[18] S.Y. Kim, G. Ahn, H.S. Kim, J.G. Je, K.N. Kim, Y.J. Jeon, Diphlorethohydroxycarmalol (DPHC) isolated from the Brown alga *Ishige okamurae* acts on inflammatory myopathy as an inhibitory agent of TNF-α, Mar. Drugs 18 (2020) 529, https://doi.org/10.3390/md18110529.

[19] C. Park, H. Lee, S.H. Hong, J.H. Kim, S.K. Park, J.W. Jeong, G.Y. Kim, J.W. Hyun, S.J. Yun, B.W. Kim, W.J. Kim, Y.H. Choi, Protective effect of diphlorethohydroxycarmalol against oxidative stress-induced DNA damage and apoptosis in retinal pigment epithelial cells, Cutan. Ocul. Toxicol. 38 (2019) 298–308, https://doi.org/10.1080/15569527.2019.1613425.

[20] D.P. Nagahawatta, N.M. Liyanage, J.G. Je, H.H.A.C.K. Jayawardhana, T.U. Jayawardena, S.H. Jeong, H.J. Kwon, C.S. Choi, Y.J. Jeon, Polyphenolic compounds isolated from marine algae attenuate the replication of SARS-CoV-2 in the host cell through a multi-target approach of $3CL^{pro}$ and PL^{pro}, Mar. Drugs 20 (2022) 786, https://doi.org/10.3390/md20120786.

[21] B. Wu, E.Y. Chien, C.D. Mol, G. Fenalti, W. Liu, V. Katritch, R. Abagyan, A. Brooun, P. Wells, F.C. Bi, D.J. Hamel, P. Kuhn, T.M. Handel, V. Cherezov, R. C. Stevens, Structures of the CXCR4 chemokine GPCR with small-molecule and cyclic peptide antagonists, Science 330 (2010) 1066–1071, https://doi.org/10.1126/science.1194396.

[22] G.A. Limb, T.E. Salt, P.M. Munro, S.E. Moss, P.T. Khaw, In vitro characterization of a spontaneously immortalized human Müller cell line (MIO-M1), Investig. Ophthalmol. Vis. Sci. 43 (2002) 864–869.

[23] I. Iandiev, A. Wurm, M. Hollborn, P. Wiedemann, C. Grimm, C.E. Remé, A. Reichenbach, T. Pannicke, A. Bringmann, Müller cell response to blue light injury of the rat retina, Investig. Ophthalmol. Vis. Sci. 49 (2008) 3559–3567, https://doi.org/10.1167/iovs.08-1723.

[24] I. Palazzo, L.J. Todd, T.V. Hoang, T.A. Reh, S. Blackshaw, A.J. Fischer, NFkB-signaling promotes glial reactivity and suppresses Müller glia-mediated neuron regeneration in the mammalian retina, Glia 70 (2022) 1380–1401, https://doi.org/10.1002/glia.24181.

[25] Palazzo L.A. Remington, D. Goodwin, Clinical Anatomy and Physiology of the Visual System E-Book, Elsevier Health Sciences, 2021.

[26] A.F. Ojeda, R.P. Munjaal, P.Y. Lwigale, Expression of CXCL12 and CXCL14 during eye development in chick and mouse, Gene Expr, Patterns 13 (2013) 303–310, https://doi.org/10.1016/j.gep.2013.05.006.

[27] A.B. Sanchez, K.E. Medders, R. Maung, P. Sánchez-Pavón, D. Ojeda-Juárez, M. Kaul, CXCL12-induced neurotoxicity critically depends on NMDA receptor-gated and L-type Ca^{2+} channels upstream of p38 MAPK, J. Neuroinflammation 13 (2016) 252, https://doi.org/10.1186/s12974-016-0724-2.

[28] C. Grimm, A. Wenzel, T. Williams, P. Rol, F. Hafezi, C. Remé, Rhodopsin-mediated blue-light damage to the rat retina: effect of photoreversal of bleaching, Investig. Ophthalmol. Vis. Sci. 42 (2001) 497–505.

[29] Y.M. Shang, G.S. Wang, D.H. Sliney, C.H. Yang, L.L. Lee, Light-emitting-diode induced retinal damage and its wavelength dependency *in vivo*, Int. J. Ophthalmol. 10 (2017) 191–202, https://doi.org/10.18240/ijo.2017.02.03.

[30] C. Roehlecke, U. Schumann, M. Ader, L. Knels, R.H. Funk, Influence of blue light on photoreceptors in a live retinal explant system, Mol. Vis. 17 (2011) 876–884.

[31] I. Jaadane, G. Villalpando Rodriguez, P. Boulenguez, S. Carré, I. Dassieni, C. Lebon, S. Chahory, F. Behar-Cohen, C. Martinsons, A. Torriglia, Retinal phototoxicity and the evaluation of the blue light hazard of a new solid-state lighting technology, Sci. Rep. 10 (2020) 6733, https://doi.org/10.1038/s41598-020-63442-5.

[32] M. Pekny, M. Nilsson, Astrocyte activation and reactive gliosis, Glia 50 (2005) 427–434, https://doi.org/10.1002/glia.20207.

[33] L.F. Sanhueza Salas, A. García-Venzor, N. Beltramone, C. Capurro, D. Toiber, D.M. Silberman, Metabolic imbalance effect on retinal müller glial cells reprogramming capacity: involvement of histone deacetylase SIRT6, Front. Genet. 12 (2021) 769723, https://doi.org/10.3389/fgene.2021.769723.

[34] I. Palazzo, K. Deistler, T.V. Hoang, S. Blackshaw, A.J. Fischer, NF-κB signaling regulates the formation of proliferating Müller glia-derived progenitor cells in the avian retina, Development 147 (2020) dev183418, https://doi.org/10.1242/dev.183418.

[35] A. Mecchia, C. Palumbo, A. De Luca, D. Sbardella, A. Boccaccini, L. Rossi, M. Parravano, M. Varano, A.M. Caccuri, High glucose induces an early and transient cytoprotective autophagy in retinal Müller cells, Endocrine 77 (2022) 221–230, https://doi.org/10.1007/s12020-022-03079-8.

[36] I. Palazzo, L.J. Todd, T.V. Hoang, T.A. Reh, S. Blackshaw, A.J. Fischer, NFkB-signaling promotes glial reactivity and suppresses Müller glia-mediated neuron regeneration in the mammalian retina, Glia 70 (2022) 1380–1401, https://doi.org/10.1002/glia.24181.

[37] K. Zeng, Y. Wang, N. Yang, D. Wang, S. Li, J. Ming, J. Wang, X. Yu, Y. Song, X. Zhou, B. Deng, X. Wu, L. Huang, Y. Yang, Resveratrol inhibits diabetic-induced müller cells apoptosis through MicroRNA-29b/specificity protein 1 pathway, Mol. Neurobiol. 54 (2017) 4000–4014, https://doi.org/10.1007/s12035-016-9972-5.

[38] Z.F. Zuo, Q. Zhang, X.Z. Liu, Protective effects of curcumin on retinal Müller cell in early diabetic rats, Int. J. Ophthalmol. 6 (2013) 422–424, https://doi.org/10.3980/j.issn.2222-3959.2013.04.02.

[39] L. Wang, H.S. Kim, J.Y. Oh, J.G. Je, Y.J. Jeon, B. Ryu, Protective effect of diphlorethohydroxycarmalol isolated from Ishige okamurae against UVB-induced damage in vitro in human dermal fibroblasts and in vivo in zebrafish, Food Chem. Toxicol. 136 (2020) 110963, https://doi.org/10.1016/j.fct.2019.110963.

[40] A. Azzi, K.J. Davies, F. Kelly, Free radical biology - terminology and critical thinking, FEBS Lett. 558 (2004) 3–6, https://doi.org/10.1016/s0014-5793(03)01526-6.

[41] C. Feillet-Coudray, T. Sutra, G. Fouret, J. Ramos, C. Wrutniak-Cabello, G. Cabello, J.P. Cristol, C. Coudray, Oxidative stress in rats fed a high-fat high-sucrose diet and preventive effect of polyphenols: involvement of mitochondrial and NAD(P)H oxidase systems, Free Radic. Biol. Med. 46 (2009) 624–632, https://doi.org/10.1016/j.freeradbiomed.2008.11.020.

[42] M. Son, D.Y. Kim, C.H. Kim, Disease modeling of rare neurological disorders in zebrafish, Int. J. Mol. Sci. 23 (2022) 3946, https://doi.org/10.3390/ijms23073946.

[43] P.F. Hitchcock, P.A. Raymond, The teleost retina as a model for developmental and regeneration biology, Zebrafish 1 (2004) 257–271, https://doi.org/10.1089/zeb.2004.1.257.

[44] D.C. Otteson, P.F. Hitchcock, Stem cells in the teleost retina: persistent neurogenesis and injury-induced regeneration, Vis. Resour. 43 (2003) 927–936, https://doi.org/10.1016/s0042-6989(02)00400-5.